

Polarization effects in one-photon free-free absorption

Philip W. Coulter

Department of Physics and Astronomy, The University of Alabama, University, Alabama 35486

S. N. Mian*

Department of Chemistry and Department of Physics and Astronomy, The University of Alabama, University, Alabama 35486

Burke Ritchie

Department of Chemistry, The University of Alabama, University, Alabama 35486

(Received 15 July 1983)

A relativistic formalism is used to include spin-orbit coupling in calculating cross sections and polarizations for one-photon free-free absorption of electrons scattering from mercury. A local exchange approximation and phenomenological polarization potential are used in the calculations. The scattering amplitudes are computed exactly. Off-shell effects are found to be important in determining the polarization of the scattered electrons. Polarizations in excess of 95% are found for some directions in the energy region where phase shifts are changing rapidly. Polarizations and off-shell effects are smaller where the phase shifts are slowly varying.

I. INTRODUCTION

There has been considerable experimental and theoretical interest in the Fano effect:^{1,2} the production of spin-polarized electrons by photoionization of unpolarized atoms using circularly polarized light. The polarization is a result of the spin-orbit interaction between the ejected electron and the atom. This effect is especially important in high- Z targets. The influence of the spin-orbit interaction has previously been studied by Fermi³ for the discrete spectrum, and Seaton⁴ for the continuum. Although the spin-orbit interaction is weak, it can cause a high degree of polarization of the ejected electrons. In Fano's original theory¹ and its experimental verification,² this phenomenon was explained as a manifestation of a Cooper minimum on the photoproduction cross section. Later studies⁵ were to show that the presence of autoionizing channels in the photoelectron continuum⁶ strongly favors the production of highly polarized electrons ejected from atoms other than alkali metals. More recently,⁷ experimental evidence for the effect of photoionization of the nS^2 atomic subshell with unpolarized light leading to a high degree of polarization has also been reported. In particular, measurements have been made of the polarization of photoelectrons ejected from mercury ($6S^2$) atoms by ultraviolet radiation. The spin polarization is believed to depend essentially on the phase-shift difference between $\epsilon P_{1/2}$ and $\epsilon P_{3/2}$ continua.

The spin polarization of electrons scattered elastically from atoms has long been the focus of theoretical and experimental considerations.⁸ The scattering of low-energy electrons from a heavy atom particularly necessitates the relativistic formulation⁹ which naturally incorporates the spin-orbit coupling to account for the spin flip of electrons. At low energy, exchange effects between the incident electron and the bound electrons, as well as the polarization of the target, must be taken into account. The spin polarization of a scattering beam of electrons in-

teracting simultaneously with an atom and an external radiation field has not been calculated previously. Moreover, the calculations are generally limited to the on-shell approximation.

It is the purpose of this paper to investigate polarization effects in free-free absorption. Photoabsorption by an electron as it is scattered by a target (i.e., inverse bremsstrahlung) has recently been studied both for an electron beam¹⁰ and an electron swarm.¹¹ In our recent work¹² it has been shown that an analog of the Fano effect does exist in free-free radiative absorption. In this paper we consider the polarization of low-energy electrons scattering from a heavy spinless target (e -Hg) due to one-photon absorption. The formulation is relativistic and includes a local exchange potential¹³ as well as a polarization potential. We present numerical calculations of differential scattering cross sections and polarization. Off-shell effects play an important role in determining the polarization of the scattered electrons.

The formalism is developed in Sec. II. The results of calculation are presented and discussed in Sec. III. Finally, Sec. IV includes the conclusions.

II. FORMALISM

We assume that the electron is described by the Hamiltonian

$$H = H_0 + H_I \quad (1)$$

where

$$H_0 = c \vec{\alpha} \cdot \vec{p} + \beta mc^2 + V(\vec{r}) \quad (2)$$

and

$$H_I = -e \vec{\alpha} \cdot \vec{A}(\vec{r}, t). \quad (3)$$

$V(\vec{r})$ is the potential for the electron-atom interaction and \vec{A} is the vector potential for the laser field which we treat

classically using a box normalization:

$$\vec{A}(\vec{r}, t) = V^{-1/2} (A_0 \vec{\lambda} e^{i(\vec{k} \cdot \vec{r} - \omega t)} + \text{c.c.}) . \quad (4)$$

λ is a unit polarization vector for the laser field.

We use the usual time-dependent theory to obtain a transition rate.¹⁴ The rate for one-photon absorption for an electron scattered into a solid angle $d\Omega$ is ($p = \hbar k$)

$$d\Gamma_A = \frac{I\alpha}{2\pi E_p^2} \frac{m}{\hbar^3} \frac{a_0^4 p_f}{V} |\mathcal{M}_{fi}|^2 d\Omega . \quad (5)$$

α is the fine-structure constant, a_0 is the Bohr radius, p_f is the final electron momentum, E_p is the photon energy expressed in hartrees, and the radiation intensity is

$$I = \frac{\omega^2 A_0^2}{2\pi c V} .$$

In the dipole approximation

$$\mathcal{M}_{fi} = \frac{mc}{\hbar} V \langle \psi_f^{(-)} | \vec{\alpha} \cdot \vec{\lambda} | \psi_i^{(+)} \rangle . \quad (6)$$

$\psi_i^{(+)}$ and $\psi_f^{(-)}$ are the initial incoming and final outgoing states of the electron, respectively, for electron-atom scattering in the absence of the laser. They are eigenstates of H_0 . The absorption cross section is obtained by dividing $d\Gamma_A$ by the incident electron flux:

$$\frac{d\sigma_A}{d\Omega} = \frac{I\alpha}{2\pi E_p^2} \frac{m^2 a_0^4}{\hbar^3} \frac{p_f}{p_i} |\mathcal{M}_{fi}|^2 . \quad (7)$$

If we make the transition to a continuum normalization, the wave functions may be computed from the Lippmann-Schwinger equation

$$\begin{aligned} \psi_{\vec{p},s}^{(\pm)}(\vec{r}) = & w(\vec{p},s) e^{i\vec{p} \cdot \vec{r} / \hbar} \\ & + \int d^3 r' \int \frac{d^3 p'}{(2\pi\hbar)^3} \frac{e^{i\vec{p}' \cdot (\vec{r} - \vec{r}') / \hbar}}{E - c\vec{\alpha} \cdot \vec{p}' - \beta mc^2 \pm i\epsilon} \\ & \times V_E(\vec{r}') \psi_{\vec{p}',s}^{(\pm)}(\vec{r}') , \end{aligned} \quad (8)$$

where $E^2 = p^2 c^2 + m^2 c^4$. In doing the calculations we use a local approximation for exchange effects.¹³ In this approximation the potential is energy dependent and requires for its computation the atomic electron density. This is taken from the Dirac-Fock calculations of Mann.¹⁵ The $w(\vec{p},s)$ are positive-energy solutions to the free-particle Dirac equation:

$$w(\vec{p},s) = \left[\frac{E + mc^2}{2mc^2} \right]^{1/2} \begin{bmatrix} \chi_s \\ \frac{c\vec{\sigma} \cdot \vec{p}}{E + mc^2} \chi_s \end{bmatrix} , \quad (9)$$

where $\chi_{1/2} = \begin{pmatrix} 1 \\ 0 \end{pmatrix}$ and $\chi_{-1/2} = \begin{pmatrix} 0 \\ 1 \end{pmatrix}$. We define the off-shell scattering amplitudes by

$$F_{s',s}(\vec{k}', \vec{k}) = - \frac{2m}{4\pi\hbar^2} \langle w(\vec{p}',s') e^{i\vec{k}' \cdot \vec{r}'} | V_E(\vec{r}) | \psi_{\vec{p},s}^{(+)}(\vec{r}) \rangle . \quad (10)$$

If the potential is invariant under time reversal and parity, then

$$F_{-s,s'}(\vec{k}, \vec{k}') = - \frac{(-1)^{1-s-s'}}{4\pi\hbar^2} \langle \psi_{\vec{p}',s'}^{(-)}(\vec{r}') | V_E(\vec{r}) | w(\vec{p},s) e^{i\vec{k} \cdot \vec{r}} \rangle . \quad (11)$$

We can use the off-shell scattering amplitudes to obtain an expression for \mathcal{M}_{fi} in the dipole approximation. The result is

$$\begin{aligned} \mathcal{M}(\vec{k}', s'; \vec{k}, s) = & \frac{2\pi a_0^2}{E_p} \frac{2mc^2}{E + E'} \vec{\lambda} \cdot [\vec{k}' F_{s',s}(\vec{k}', \vec{k}) - (-1)^{1-s-s'} \vec{k} F_{-s,-s'}(\vec{k}, \vec{k}')] \\ & + \frac{2}{\pi} \sum_{s''} (-1)^{1-s-s''} \int d^3 k'' \vec{\lambda} \cdot \vec{k}'' \frac{F_{-s'',-s'}(\vec{k}'', \vec{k}') F_{s'',s}(\vec{k}'', \vec{k})}{(k'^2 - k''^2 + i\epsilon)(k^2 - k''^2 + i\epsilon)} . \end{aligned} \quad (12)$$

This has the same form as the nonrelativistic expression¹² in the limit $2mc^2/(E + E') \rightarrow 1$.

We expand the wave function as

$$w(\vec{p},s) e^{i\vec{k} \cdot \vec{r}} = \left[\frac{E + mc^2}{2mc^2} \right]^{1/2} \sum_{J,M} \sum_{l,m} 4\pi i^l (lm; \frac{1}{2}s | l\frac{1}{2}; JM) Y_{lm}^*(\hat{k}) \begin{bmatrix} j_l(kr) \mathcal{Y}_{JM}^l(\hat{r}) \\ g_{Jl}(kr) \frac{\vec{\sigma} \cdot \vec{r}}{r} \mathcal{Y}_{JM}^l(\hat{r}) \end{bmatrix} , \quad (13)$$

$$\psi_{\vec{p},s}^{(+)}(\vec{r}) = \left[\frac{E + mc^2}{2mc^2} \right]^{1/2} \sum_{J,M} \sum_{l,m} 4\pi i^l (lm; \frac{1}{2}s | l\frac{1}{2}; JM) Y_{lm}^*(\vec{k}) \begin{bmatrix} F_{Jl}(k,r) \mathcal{Y}_{JM}^l(\hat{r}) \\ G_{Jl}(k,r) \frac{\vec{\sigma} \cdot \vec{r}}{r} \mathcal{Y}_{JM}^l(\hat{r}) \end{bmatrix} . \quad (14)$$

j_l is a spherical Bessel function of the first kind,

$$g_{Jl}(kr) = -\frac{i\hbar c}{E+mc^2} \left[\frac{\partial}{\partial r} + \frac{1+\kappa}{r} \right] j_l(kr), \quad (15)$$

$$G_{Jl}(k,r) = -\frac{i\hbar c}{E+mc^2-V(r)} \left[\frac{\partial}{\partial r} + \frac{1+\kappa}{r} \right] F_{Jl}(k,r), \quad (16)$$

$$\kappa = -J(J+1) + l(l+1) - \frac{1}{4}, \quad (17)$$

and

$$\mathcal{Y}_{JM}^l(\hat{r}) = \sum_{m,s} (lm; \frac{1}{2}s \mid l\frac{1}{2}; JM) Y_{lm}(\hat{r}) \chi_s. \quad (18)$$

Using these expansions we find that

$$F_{s',s}(\vec{k}', \vec{k}) = -\frac{8\pi m}{\hbar^2} \left[\frac{(E+mc^2)(E'+mc^2)}{(2mc^2)^2} \right]^{1/2} \times \sum_{J,M,l} (l, M-s'; \frac{1}{2}s' \mid l\frac{1}{2}; JM) (l, M-s; \frac{1}{2}s \mid l\frac{1}{2}; JM) v_{Jl}(k', k) Y_{l, M-s'}(\hat{k}') Y_{l, M-s}^*(\hat{k}), \quad (19)$$

where

$$v_{Jl}(k', k) = \int_0^\infty r^2 dr [j_l(k'r) V_E(r) F_{Jl}(k, r) + g_{Jl}(k'r) V_E(r) G_{Jl}(k, r)]. \quad (20)$$

We can now obtain an exact expression for $\mathcal{M}(k's', k, s)$ in terms of off-shell matrix elements for electron-atom scattering. If we define

$$Q_{Jl, J'l'}(k', k) = \int_0^\infty \frac{E''+mc^2}{2mc^2} \frac{k''^3 dk''}{(k'^2 - k''^2 + i\epsilon)(k^2 - k''^2 + i\epsilon)} v_{Jl}(k'', k') v_{J'l'}(k'', k) \quad (21)$$

then

$$\begin{aligned} \mathcal{M}(\vec{k}', s'; \vec{k}, s) = & -\frac{16\pi^2 a_0^2}{\hbar^2 E_p} \frac{2mc^2}{E+E'} \left[\frac{(E+mc^2)(E'+mc^2)}{(2mc^2)^2} \right]^{1/2} \\ & \times \sum_{J,l,M} (l, M-s'; \frac{1}{2}s' \mid l\frac{1}{2}; JM) (l, M-s; \frac{1}{2}s \mid l\frac{1}{2}; JM) \\ & \times \vec{\lambda} \cdot [\vec{k}' v_{Jl}(k', k) - \vec{k} v_{Jl}(k, k')] Y_{l, M-s'}(\hat{k}') Y_{l, M-s}^*(\hat{k}) \\ & + \frac{2}{\pi} \left[\frac{8\pi m}{\hbar^2} \right]^2 \left[\frac{(E+mc^2)(E'+mc^2)}{(2mc^2)^2} \right]^{1/2} \sum_{\substack{J,l,M, \\ J',l',m}} \left[\frac{(2l+1)(2l'+1)(2J+1)(2J'+1)}{3} \right]^{1/2} \\ & \times (-1)^{s-s'+M+Y_2} \begin{Bmatrix} 1 & l & l' \\ 0 & 0 & 0 \end{Bmatrix} \begin{Bmatrix} J & \frac{1}{2} & l \\ l' & 1 & J' \end{Bmatrix} (l, M-s'; \frac{1}{2}s' \mid l\frac{1}{2}; JM) \\ & \times (l', M+m-s; \frac{1}{2}s \mid l'\frac{1}{2}; J'M+m) \\ & \times (JM; J'-M-m \mid JJ'; 1-m) \lambda_m \\ & \times Y_{l, M-s'}(\hat{k}') Y_{l', M+m-s}^*(\hat{k}) Q_{Jl, J'l'}(k', k). \quad (22) \end{aligned}$$

In this paper we compute off-shell scattering amplitudes at energies up to a few electron volts. Thus we can make the approximations of setting $E = mc^2$ and neglecting the lower components of the wave functions. In the nonrelativistic limit

$$v_{Jl}(k', k) = \int_0^\infty r^2 dr j_l(k'r) V_E(r) F_{Jl}(k, r) \quad (23)$$

and

$$\begin{aligned} Q_{Jl; J'l'}(k', k) &= \int_0^\infty \frac{k''^3 dk''}{(k'^2 - k''^2 + i\epsilon)(k^2 - k''^2 + i\epsilon)} \\ &\quad \times v_{Jl}(k'', k') v_{J'l'}(k'', k). \end{aligned} \quad (24)$$

The integration over k'' in Eq. (24) is slowly convergent, but fortunately this integration can be done exactly. By using Eq. (23) we see that $Q_{Jl; J'l'}$ can be written as

$$\begin{aligned} Q_{Jl; J'l'}(k', k) &= \int_0^\infty r^2 dr \int_0^\infty r'^2 dr' F_{Jl}(k, r) V_E(r) V_E(r') \\ &\quad \times F_{J'l'}(k'r') H_{ll'}(k'k; r'r), \end{aligned} \quad (25)$$

where

$$\begin{aligned} H_{ll'}(k', k; r'r) &= \int_0^\infty \frac{k''^3 dk''}{(k'^2 - k''^2 + i\epsilon)(k^2 - k''^2 + i\epsilon)} \\ &\quad \times j_l(k''r) j_{l'}(k''r') \end{aligned} \quad (26)$$

can be evaluated exactly by rewriting it as a contour integral in the complex k'' plane. Note that l and l' differ by one because of the factor $\begin{pmatrix} l & l' \\ 0 & 0 \end{pmatrix}$ in Eq. (22).

Our results for the differential cross section are presented by factoring out the dependence on the laser intensity and the electron density. Using Eq. (5) we define a differential absorption cross section by

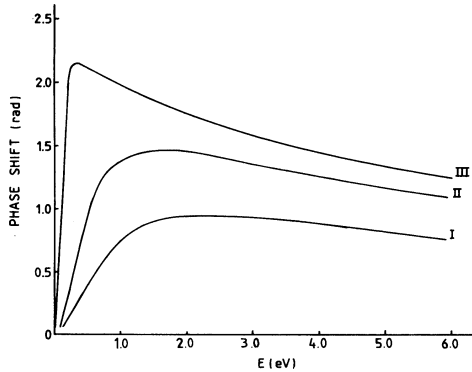


FIG. 1. Phase shifts for e -Hg scattering as a function of incident energy. I corresponds to spin up ($P_{3/2}$). II corresponds to spin down ($P_{1/2}$). III is also spin down ($P_{1/2}$) but includes the polarization potential.

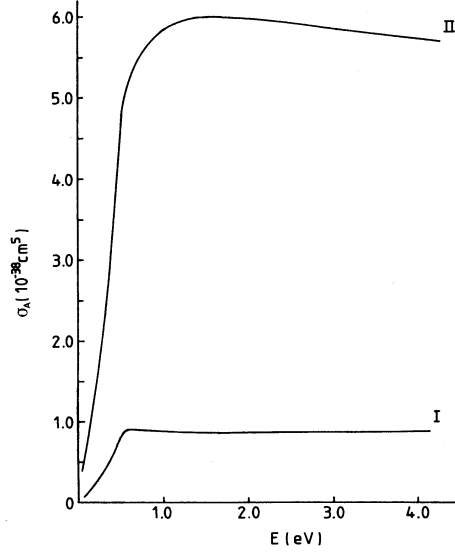


FIG. 2. Differential cross section for e -Hg scattering with one-photon absorption ($E_p = 0.62$ eV) as a function of incident electron energy for $\theta = 45^\circ$. I represents scattering in the xz plane and II in the yz plane.

$$\frac{d\Gamma_A}{d\Omega} = FN\sigma_A(\theta, \varphi), \quad (27)$$

where $F = I/(\hbar\omega)$ is the photon flux in $\text{cm}^{-2}\text{s}^{-1}$ and $N = V^{-1}$ is the number of electrons per unit volume. Hence

$$\sigma_A(\theta, \varphi) = \frac{a_0}{2\pi mc E_p} \frac{P_f}{\hbar} |\mathcal{M}_{fi}|^2. \quad (28)$$

σ_A has units of cm^5 . We assume here that the incident electrons are traveling in the positive z direction and that the laser field is polarized along the x axis. The cross sections which we show are obtained by averaging over the initial electron polarizations and summing over the final polarization.

If we suppress the momenta and write $\mathcal{M}_{\pm\pm} = \mathcal{M}(\vec{k}' \pm \frac{1}{2}; \vec{k} \pm \frac{1}{2})$ the polarization components are

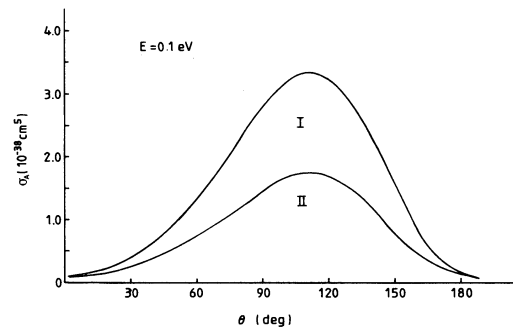


FIG. 3. Differential cross section for e -Hg scattering with one-photon absorption ($E_p = 0.62$ eV) at 0.1 eV incident energy as a function of θ . I represents scattering in the yz plane and II in the xz plane.

$$\begin{aligned}
 P_x &= 2 \frac{\text{Re}(\mathcal{M}_{++} \mathcal{M}_{-+}^* + \mathcal{M}_{+-} \mathcal{M}_{--}^*)}{\sum_{m,m'} |\mathcal{M}_{mm'}|^2}, \\
 P_y &= -2 \frac{\text{Im}(\mathcal{M}_{++} \mathcal{M}_{-+}^* + \mathcal{M}_{+-} \mathcal{M}_{--}^*)}{\sum_{m,m'} |\mathcal{M}_{mm'}|^2}, \\
 P_z &= \frac{|\mathcal{M}_{++}|^2 + |\mathcal{M}_{+-}|^2 - |\mathcal{M}_{--}|^2 - |\mathcal{M}_{-+}|^2}{\sum_{m,m'} |\mathcal{M}_{mm'}|^2}.
 \end{aligned} \quad (29)$$

The component perpendicular to the scattering plane is

$$P_{\perp} = -P_x \sin\varphi + P_y \cos\varphi. \quad (30)$$

We note that if off-shell effects are neglected, the component of polarization along the beam direction is zero.

III. RESULTS AND DISCUSSION

Recent theoretical investigations^{16,17} of low-energy electron scattering from mercury have shown that the polarization potential resulting from atomic distortion makes an

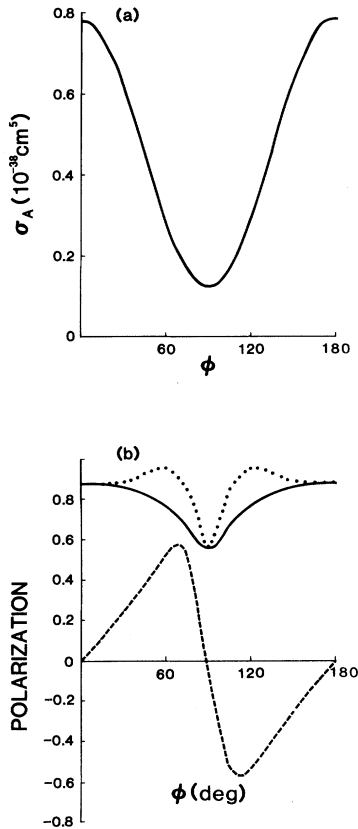


FIG. 4. (a) Differential absorption cross section ($E_p=0.62$ eV) for e -Hg scattering as a function of azimuthal angle. (b) Polarization as a function of azimuthal angle. Dashed curve represents polarization along the direction of the scattered electron (P_k). Solid curve represents the polarization component perpendicular to the scattering plane (P_{\perp}). Dotted curve is the magnitude of the polarization. Incident energy is 0.1 eV and $\theta=45^\circ$.

important contribution to phase shifts and cross sections. The potential is proportional to r^{-4} at large distances from the atom.¹⁸ We have included this potential in our calculation and have chosen it to be of the form¹⁹ $V_p(r) = -0.5\alpha r^2(r^2 + r_0^2)^{-3}$. α is the static dipole polarizability of Hg. 5.1 \AA^3 is believed to be its most reliable value.²⁰ The presence of the cutoff distance r_0 ensures that the potential remains finite at small r ; it is, however, very sensitive to the variation of r_0 . Relativistic phase-shift calculations give two sets of values corresponding to spin up and spin down. The spin-down phase shift is larger because the potential is more attractive. Thus in Fig. 1, the $P_{1/2}$ phase-shift curve lies higher and possesses a broad maximum. On including the polarization potential and considering some variation of r_0 , the calculated $P_{1/2}$ phase shift shows resonant behavior (Fig. 1). For $r_0=1.693 \text{ \AA}$, the phase shift increases sharply and attains a maximum at a much lower energy value ($E=0.3$ eV). Sin Fai Lam¹⁷ obtained a similar curve having the peak centered at $E \approx 0.25$ eV with the second-order Dirac potential, and at $E \approx 0.35$ eV with the Pauli approximation used in his calculation.

The integrals defined in Eqs. (23) and (25), respectively, were evaluated numerically [$J'=l' \pm \frac{1}{2}$; + (-) sign represents spin up (down)] using the dipole selection rule

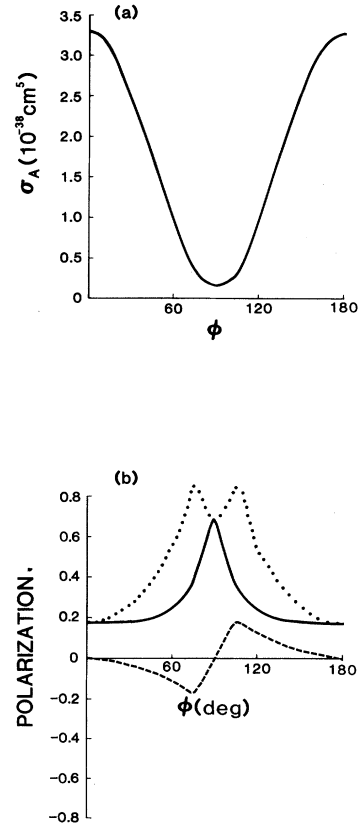


FIG. 5. (a) Differential absorption cross section ($E_p=0.62$ eV) for e -Hg scattering as a function of azimuthal angle. (b) Polarization as a function of azimuthal angle. Notation is the same as in Fig. 4. Incident energy is 0.1 eV and $\theta=105^\circ$.

$|l'-l|=1$ which emerges from the 3- j symbol present as an overall multiplicative factor in the expression for the transition amplitude. These integrals were used in the partial-wave expansion to compute the scattering amplitude from Eq. (22) for given initial and final spin orientations and the spatial direction of the scattered electron. For low-energy scattering, though the most significant contribution results from the p -wave, we have carried out the partial-wave summation through d waves ($l=2$). Differential inelastic scattering cross sections and the polarizations are calculated corresponding to various angular directions ($\theta=0^\circ, 15^\circ, \dots, 180^\circ$; $\phi=0^\circ, 15^\circ, \dots, 360^\circ$) of the scattered beam at different incident energy values from $E=0.1$ to $E=3.5$ eV.

Figure 2 shows the energy dependence of the cross section for an electron scattering after the absorption of a single photon ($E_p=0.62$ eV). It has been shown for laser radiation linearly polarized in a direction perpendicular to the incident electron beam that the on-shell cross section is proportional to $\cos^2\phi$ and should be zero for scattering in the yz plane.¹² The inclusion of off-shell effects results in a nonzero cross section [Eq. (46) of Ref. 12] which is expected to be small.²¹ Comparing the cross section in the yz plane with that in the xz plane confirms this prediction. At higher energy it is seen that in the former case the cross section is about one sixth the corresponding value for scattering in the latter ($\theta=45^\circ$) which has both off-shell and on-shell contributions. In the forward as well as

in the backward directions the effect on scattering is entirely due to off-shell contributions. As the energy increases (up to $E=3.5$ eV) the forward scattering shows a gradual increase whereas the backward scattering, as expected, tends to decrease beyond the incident energy $E=0.5$ eV. At $E=0.1$ eV the cross section in the xz plane attains a maximum (for about $\theta=110^\circ$) which decreases to lower values as the plane of scattering becomes coincident with the yz plane (Fig. 3).

Off-shell effects play an important role in determining the polarization of the scattered electrons. In Figs. 4, 5, and 6 we show the components of polarization perpendicular to the scattering plane (P_\perp) and parallel to the scattered electron momentum (P_k) for selected values of θ and E . The magnitude of the polarization is also shown. If off-shell effects are neglected, only P_\perp is nonzero.¹² It is clear from the graphs that off-shell effects must be considered in computing the spin polarization of the scattered electrons.

In Fig. 4 we show the polarization and the cross section as a function of azimuthal angle for $E=0.1$ eV and $\theta=45^\circ$. This is in the resonant region where we expect polarization and off-shell effects to be large. We note that the polarization remains large ($\approx 88\%$) where the cross section is maximal. This is in contrast to the Fano effect and polarization by elastic scattering where large polarizations are associated with small cross sections. The maximum differential cross section for $E=0.1$ eV occurs near $\theta=105^\circ$ (Fig. 5). At this angle the polarization is minimal ($\approx 18\%$) where the cross section is largest. From Fig. 6 we see that the maximum polarization decreases significantly

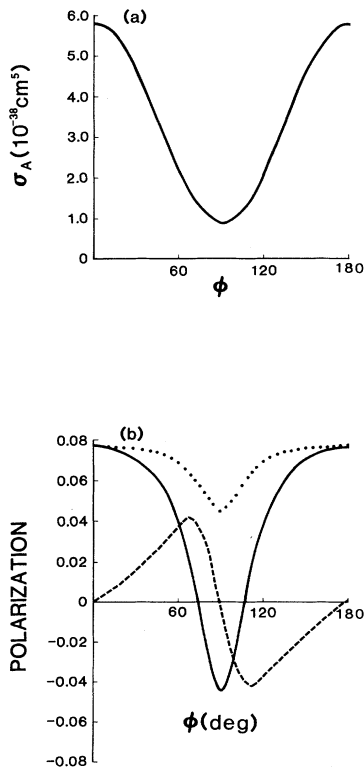


FIG. 6. (a) Differential absorption cross section ($E_p=0.62$ eV) for e -Hg scattering as a function of azimuthal angle. (b) Polarization as function of azimuthal angle. Notation is the same as in Fig. 4. Incident energy is 3.5 eV and $\theta=45^\circ$.

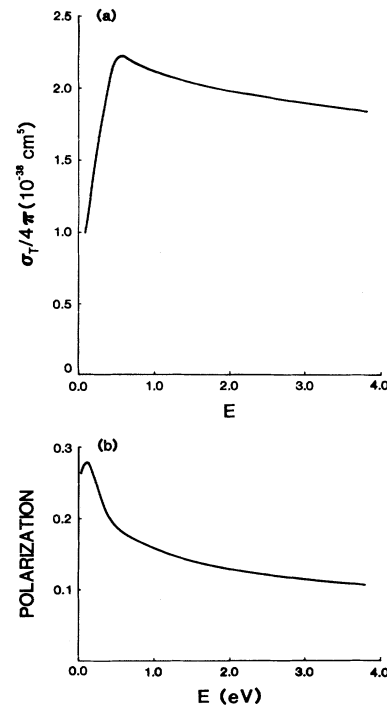


FIG. 7. (a) Total absorption cross section ($\sigma_T/4\pi$) as a function of incident energy. (b) Average polarization perpendicular to the scattering plane as a function of the incident energy.

cantly in the non-resonant region ($E = 3.5$ eV).

In Fig. 7 we plot the total cross section and the average component of polarization perpendicular to the scattering plane as a function of energy. The average polarization decreases rapidly away from the resonant region.

Assuming the off-shell contribution to the amplitude to be 10% Coulter and Ritchie¹² found that the polarization along the incident beam direction becomes large in the region $\phi = 80^\circ$ for some fixed θ . The present calculation shows that the polarization is maximal (84%) for $\theta = 105^\circ$ at $\phi \approx 75^\circ$. P_z makes the major contribution to the polarization here. The cross section is relatively small in this direction (Fig. 6). The fact that the magnitude of the maximum is larger here indicates that the off-shell contribution exceeds 10%. This is not unexpected in view of the resonant behavior for low-energy electron scattering from mercury.^{17,22} Walker²² has pointed out that the resonance occurs only if the effects of atomic distortion produced by the electrostatic field of the incident electron are included. The resonance is not sharp, however, because the excitation of the target electrons is to a large number of states rather than to a discrete one.

IV. CONCLUSION

The cross section and the polarization components for one-photon absorption by a low-energy electron scattering

from Hg atoms have been obtained using a relativistic formulation. For scattering in the yz plane (including the forward and the backward directions) the cross section is entirely due to the off-shell contributions. The off-shell effects completely determine the polarization of electrons along the incident beam direction. If the scattering occurs in an arbitrary direction, the on-shell and the off-shell effects together give rise to both the cross section and the polarization perpendicular to the scattering plane. At higher energy ($E > 1.0$ eV) and $\theta = 45^\circ$, the off-shell contribution to the cross section (yz plane) is one sixth the corresponding value of the cross section if the scattered direction lies in the xz plane. No polarization occurs if the electrons scatter in the forward or the backward direction. At low energy and for specific directions of scattering, an incident unpolarized beam of electrons can emerge with any component of polarization having a magnitude greater than 0.7.

ACKNOWLEDGMENTS

It is a pleasure to acknowledge the donors of the Petroleum Research Fund as administered by the American Chemical Society for their support of this research. The calculations were done at the Charles Seebeck Computer Center at The University of Alabama.

*Permanent address: Department of Physics, Ranchi University, Ranchi 834008, Bihar, India.

¹U. Fano, Phys. Rev. **178**, 131 (1969); **184**, 250 (1969).

²For a review, see J. Kessler, *Polarized Electrons* (Springer, Berlin, 1976).

³E. Fermi, Z. Phys. **52**, 680 (1929) [also in *Collected Papers of Enrico Fermi* (University of Chicago, Chicago, 1962), p. 322].

⁴M. J. Seaton, Proc. R. Soc. London, Ser. A **208**, 408 (1951), Sec. 5.

⁵U. Heinzmann, H. Heuer, and J. Kessler, Phys. Rev. Lett. **34**, 441 (1975).

⁶U. Fano, Phys. Rev. **124**, 1866 (1961).

⁷G. Schoenhense, U. Heinzmann, J. Kessler, and N. A. Cherepkov, Phys. Rev. Lett. **48**, 603 (1982).

⁸H. A. Tolhoek, Rev. Mod. Phys. **28**, 277 (1956); P. J. Bunyan and J. L. Schonfelder, Proc. Phys. Soc. London **85**, 455 (1965); S. Lin, N. Sherman, and J. K. Percus, Nucl. Phys. **45**, 492 (1963); J. Mehr, Z. Phys. **198**, 345 (1967).

⁹H. N. Browne and E. Bauer, Phys. Rev. Lett. **16**, 495 (1966);

D. W. Walker, Adv. Phys. **20**, 257 (1971) and references therein; L. T. Sin Fai Lam and W. E. Baylis, J. Phys. B **14**,

559 (1981).

¹⁰A. Weingartshofer, E. M. Clarke, J. K. Holmes, and C. Jung, Phys. Rev. A **19**, 2371 (1979).

¹¹B. Ritchie, Phys. Rev. A **23**, 2276 (1981).

¹²P. W. Coulter and B. Ritchie, Phys. Rev. A **24**, 3051 (1981).

¹³M. E. Riley and D. G. Truhlar, J. Chem. Phys. **63**, 2182 (1975).

¹⁴G. Baym, *Lectures on Quantum Mechanics* (Benjamin, New York, 1973).

¹⁵J. B. Mann, Los Alamos National Laboratory Report (unpublished).

¹⁶D. W. Walker, J. Phys. B **3**, L123 (1970); **3**, 788 (1970).

¹⁷L. T. Sin Fai Lam, Aust. J. Phys. **33**, 261 (1980).

¹⁸A. Temkin, Phys. Rev. **107**, 1004 (1957).

¹⁹W. E. Baylis, J. Phys. B **10**, L583 (1977); J. Migdalek and W. E. Baylis, Phys. Rev. A **26**, 1839 (1982).

²⁰R. R. Teachout and Russel T. Pack, At. Data **3**, 195 (1971).

²¹N. M. Kroll and K. M. Watson, Phys. Rev. A **8**, 804 (1973); F. E. Low, Phys. Rev. **110**, 974 (1958).

²²D. W. Walker, J. Phys. B **8**, L161 (1975).